Low Noise Nanometer Scale Room-Temperature $YBa_2Cu_3O_{7-x}$ Bolometers for THz Direct Detection

Stella Bevilacqua, *Student Member, IEEE*, and Sergey Cherednichenko

***Abstract*—We present a detailed investigation of the responsivity and the noise in room temperature THz direct detectors made of $YBa_2Cu_3O_{7-x}$ (YBCO) thin-film nano-bolometers. The YBCO nano-bolometers are integrated with planar spiral antennas covering a frequency range from 100 GHz to 2 THz. The detectors were characterized at 1.6 THz, 0.7 THz, 400 GHz and 100 GHz. The maximum electrical responsivity of 70 V/W and a minimum noise equivalent power (NEP) of 50 pW/Hz$^{0.5}$ were measured, whereas the highest optical responsivity was 45 V/W. The $(1/f)$ noise in nano-bolometers is independent on the device volume and can be found as $(V_N/V)^2 = 6 \times 10^{-11} \times 1/f$ Hz^{-1} for a given modulation frequency f and a dc voltage V.**

***Index Terms*—Bolometer, responsivity, room temperature operation, THz detectors, $YBa_2Cu_3O_{7-x}$ (YBCO) film.**

I. Introduction

THE continuous development of terahertz (0.1 THz–10 THz) detectors and sources is a key point for the progress of different areas of science and technology, such as security and medical imaging and probing, high resolution radar system, spectroscopy, communication etc [1], [2]. THz wave detection includes cooled as well as room temperature detector technologies. Many applications require very fast and sensitive room temperature detectors, extending their operation to several THz.

A number of room temperature detector types have been reported for frequencies below 1 THz, e.g., tunnel diodes, FET detectors and Schottky diodes [3]. Schottky diodes are the most sensitive room temperature detectors for sub-THz frequencies [4], [5] however, their sensitivity decreases significantly for frequencies above 1 THz as it is limited by the RC time constant. MOSFET detectors, based on plasma wave phenomena, have attracted large attention in the research field due to the fast response and good responsivity prospects in the THz range [6].

For frequencies over 1 THz, the most common detectors probably are Golay cells and pyroelectric detectors.[1] However, a big drawback of those is a low response rate of just a few tens of hertz (Hz). They are also bulky and do not allow for integration with on-chip systems.

Manuscript received May 14, 2014; revised June 27, 2014; accepted July 24, 2014. Date of publication August 06, 2014; date of current version October 30, 2014. This work was supported by the Swedish Research Council (VR).

The authors are with the Department of Microtechnology and Nanoscience (MC2), Chalmers University of Technology, SE-41296 Göteborg, Sweden (e-mail: stellab@chalmers.se; serguei@chalmers.se).

Color versions of one or more of the figures in this paper are available online at http://ieeexplore.ieee.org.

Digital Object Identifier 10.1109/TTHZ.2014.2344435

[1]Available: http://www.mtinstruments.com/thzdetectors

For room temperature detection bolometers thermally isolated on thin membranes have demonstrated responsivity up to several kilovolts per watt (kV/W) [7]. Despite having relatively large responsivity, disadvantages of membrane bolometers are the long response time and the complicated fabrication process.

Free-standing bridge bolometers made from Nb_5N_6 and Nb thin films coupled with planar antenna were reported in [8], [9]. Because of the weak thermal coupling with the substrate, such microbolometers have shown large responsivity. Just as membrane bolometers, free-standing bridge bolometers are known to be slow and have a rather complicated fabrication process.

Other types of antenna-coupled bolometers are substrate supported bolometers which are very sensitive at cryogenic temperature. The advantages of using substrate supported bolometers are a faster response time and an easier fabrication process compared to membrane and air-bridge bolometers.

Recently, we have demonstrated that a nanosecond response time and a high responsivity are feasible for YBCO antenna-coupled bolometers on a bulk substrate at room temperature operation [10]. There we reported that the bolometer responsivity scales inversely with the device lateral dimensions (width$\times$length), which is in agreement with the bolometer cooling into the substrate via the phonon exchange [10]. An electrical responsivity of 15 V/W and an NEP of 450 pW/Hz$^{0.5}$ was also demonstrated. Moreover, the predicted improvement of the sensitivity in nano-bolometers is preliminary presented in [11]. $PrBa_2Cu_3O_{7-x}$ films have also been shown to have good prospect for such devices [12]. With a negative Temperature Coefficient of Resistance (TCR) of 0.01-0.02 K^{-1} an electrical responsivity of 33 V/W and an electrical NEP of 150 pW/Hz$^{0.5}$ were reported.

In this work we continue to investigate the room temperature operation (20 °C) of antenna integrated nano-bolometers made of thin films of $YBa_2Cu_3O_{7-x}$ (YBCO) as direct detectors. Promising experimental results have been achieved in terms of responsivity and sensitivity of YBCO room temperature sub-micron detectors indicating a possibility to develop a far-IR multi-pixel system with a simpler fabrication and lower cost.

II. Film Deposition and Device Fabrication

The YBCO film, with a thickness of about 70 nm, was deposited using the pulsed laser deposition (PLD) technique. Despite good crystalline matching of YBCO with $SrTiO_3$ or $LaAlO_3$ [13], dual-side polished R-plane sapphire was used in our work as a substrate for YBCO deposition. The dielectric constant close to that of Si, and low absorption loss ($\varepsilon = 9.34$ and $tan\delta = 3 \times 10^{-5}$ at 77 K [13]) of sapphire are essential for the back illumination of the YBCO detector at THz frequencies.

The YBCO quality is influenced by many factors such as the interface between the film and the substrate. Because of this, it is important to properly clean the substrate before starting the deposition. Moreover, due to the large crystalline mismatch of YBCO with sapphire [13], a buffer layer is required. The deposition system used in this work is equipped with three chambers. Two of them are dedicated to metal and oxide sputtering while the third chamber is dedicated only to YBCO deposition. These three chambers are connected through a buffer line which it is kept at a base pressure of 10^{-7} mbar allowing for *in situ* multilayer depositions of different materials.

In our work a 25–30 nm buffer layer of CeO_2 was deposited using RF sputtering at substrate temperature of 750 °C and oxygen pressure of $p_{O_2} = 0.1$ mbar. After the deposition the oxygen pressure was raised to 730 mbar and the substrate was cooled down to room temperature at a rate of 10 °C/min.

For the YBCO deposition the samples were transferred into the PLD chamber. The YBCO deposition temperatures ranged from 780 °C to 855 °C, heating was applied at an oxygen pressure of $p_{O_2} = 0.6$ mbar. Pulses from a KrF laser were focused onto a rotating target and the YBCO film was deposited. After the deposition, the oxygen pressure inside the chamber was increased to 860 mbar and the sample was cooled down to 550 °C and annealed for one hour. Afterwards, the sample was cooled down to room temperature.

In order to protect the YBCO film during the patterning as well as to improve the YBCO/Au electrical contact resistance, a 20 nm *in-situ* gold layer was sputtered on top of the YBCO film.

Bolometers integrated with planar spiral antennas were fabricated by several electron-beam lithography, lift-off process and etching steps. Using double layer positive e-beam resist, metals deposition (Ti/Au/Ti), and corresponding lift-off process the bolometers length was defined using small contact pads. Then the spiral antenna, which had an overlap with the contact pads, was shaped with the same positive resist, metals deposition (Ti/Au/Ti), and lift-off process. The Ti top layer was used as etching mask during the subsequent process steps. At this stage the 20 nm *in situ* gold layer on top of YBCO was removed by wet-etching with a solution of KI:I_2 and water. As final step, negative e-beam resist was used to define the bolometer and subsequently the YBCO film was etched with Ar ion-milling in the region not protected by the resist and the Ti masks. Fig. 1 shows a scanning electron microscope (SEM) image of a YBCO device with a bolometer area of 0.09 μm^2. The negative e-beam resist, after the Ar etching, was left on top of the bolometer bridge to create a sort of passivation.

At room temperature, a rather high TCR of 0.0012–0.0025 K^{-1} makes YBCO films very suitable for THz detection. The high resistivity provides a bolometer resistance on the order of $R = 50$–$900\ \Omega$, which is suitable for integration with the majority of planar THz antennas. In general, there is no upper frequency limit for the YBCO bolometers, and efficient detection with YBCO nano-bolometers has been reported well into near IR [14], [15].

III. Experimental Setup

In this paper we will describe three sets of measurements: dc characteristics, RF responsivity, and the output noise measurements. DC measurements comprised the current-voltage $(I$–$V)$ characterization (at room temperature) and resistance versus temperature $(R$–$T)$ characterization. Both measurements were done in a dip-stick which was cooled in a liquid nitrogen transport dewar allowing for temperature variation down to 77 K.

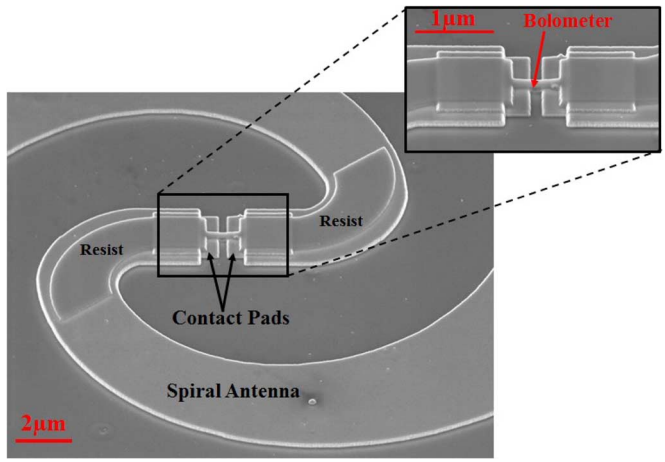

Fig. 1. SEM picture of YBCO nano-bolometer integrated with a spiral antenna on a sapphire substrate. The insert is a zoom into the antenna center with the bolometer in-between.

The optical responsivity, which is the ratio of the output voltage to the incident THz wave power, was measured at 400 GHz using a coherent multiplier based source.[2] The amplitude modulation (AM) up to 100 kHz was done via the AM modulation of the input signal (∼11 GHz) provided by an Agilent signal generator. The spiral antenna integrated YBCO nano-bolometers were clamped to the back side of a 5 mm diameter Si lenses forming a quasi-optical setup. The 400 GHz source was equipped with a 3.6 mm diagonal horn antenna with a directivity of 26 dB. The beam waist of such a horn antenna is very close to the beam waist of the detector (on the 5 mm lens). Therefore, by placing both the detector and the source at about 5 mm from each other a high coupling efficiency can be achieved. The emitted power level of the 400 GHz source was measured to be $P_{\text{out}} = 170\ \mu$W using a waveguide Erikson power meter with the same horn antenna as the source. In this case both horns were placed at about 5 mm from each other. For comparison, with both horns removed and the source and the power meter waveguides flanged together a power of about 200 μW was measured. For the responsivity calculations the optical power value of 170 μW was used referenced to the Si lens input. Since the spiral antenna is elliptically polarized (in contrast to the linearly polarized horn antenna) a loss coupling factor of 0.5 was further taken into consideration, as well as a transmission coefficient at the lens-air interface of 0.7.

The optical response of nano-bolometers was also measured at 1.6 and 0.7 THz using a far infrared (FIR) gas laser, and at 100 GHz using a Gunn diode oscillator signal sources.

The bolometer readout was done using a dual phase lock-in amplifier in series with a voltage preamplifier (noise level of approximately 0.73 nV/Hz$^{0.5}$).[3] A dc block after the detector was used to avoid saturation of the preamplifier. The voltage

[2][Online] Available: http://vadiodes.com/index.php/en

[3][Online] Available: http://www.femto.de/en

response extracted from the lock-in was then multiplied by a factor of 2 (peak-to-peak magnitude) and a factor of $\sqrt{2}$ originated from the lock-in rms amplitude and divided by the preamplifier gain. For the noise measurements the same preamplifier and lock-in amplifier with an internal reference source from 20 Hz to 100 kHz were used.

For the responsivity and the noise measurements the bolometers were current biased with a voltage source and a 10 kΩ resistor in series. With this schematic the bolometer noise was much less compared to a case when the bolometer was biased with a current stabilized source. We believe that extra noise was generated by the current control feedback loop of the current source.

IV. DC Characterization

DC (also called electrical or thermal) responsivity is an important figure-of-merit which is used to estimate the RF voltage responsivity of the bolometers. The bolometer responsivity (1) is a function of the bias current, i, the temperature coefficient of resistance (TCR), α, and the effective thermal conductance to the heat sink, G_e [16]

$$R_V = \frac{i \cdot \alpha \cdot R}{(G_e)} = \frac{i \cdot \alpha \cdot R}{G - i^2 \cdot \alpha \cdot R} \tag{1}$$

where G is the thermal conductance when no current is applied and R is the device room temperature resistance. The temperature coefficient of resistance $(\alpha = \partial R/\partial T \times 1/R)$ (1) was experimentally obtained from the resistance versus temperature, $R(T)$, measurements as explained in [10].

Previously, we discussed that the dominating heat removal process from the YBCO micro bolometers occurs into the substrate [10]. We still adhere to this hypothesis. In this case, the thermal conductance G is in direct proportion to the bolometer area A, and it is in inverse proportion to the thermal boundary resistance between the film and the substrate $R_{\rm bd}$ [17]

$$G = A/R_{\rm bd}. \tag{2}$$

The heat conductance can be obtained from (3), using a current-voltage $(I$–$V)$ and the resistance-temperature $(R$–$T)$ curves of the device

$$G \equiv \frac{\partial P_{\rm dc}}{\partial T} = \frac{\partial P_{\rm dc}}{\partial R} \cdot \frac{\partial R}{\partial T} \tag{3}$$

where $P_{\rm dc}$ is the Joule power dissipated in the (dc) current biased bolometer.

The dissipated dc power and the resistance can be extrapolated at room temperature by recording the current–voltage $(I$–$V)$ curves YBCO nano-bolometer without the RF power applied. Examples of dc power versus resistance curves are shown in Fig. 2 for two devices with dimensions of 0.3μm × 0.5μm and room temperature resistances of 950 Ω and 360 Ω. By linearly fitting the $P_{\rm dc}(R)$ data, $(\partial P_{\rm dc}/\partial R)$ was obtained (see Fig. 2). As we have shown in [10], the $(\partial R/\partial P_{\rm dc})$ is equal to the bolometer responsivity at a bias current of 1 mA if $(\partial R/\partial P_{\rm dc})$ is expressed in ohms per milliwatt (Ω/mW).

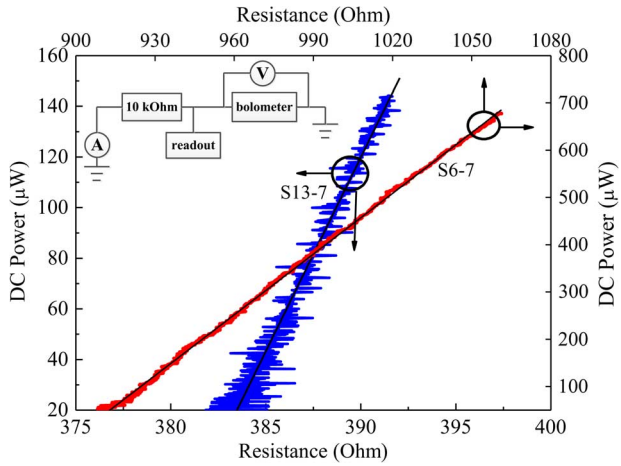

Fig. 2. The dissipated dc power as a function of the resistance for 0.3μm × 0.5μm (width and length) bolometers. Data of devices S13-7 and S6-7 are referred to primary and secondary axes respectively. The readout schematic is shown in the inset.

For the nano-bolometers from Fig. 2 electrical responsivities of 230 and 65 V/W were deduced at room temperature and at 1 mA bias current.

Devices fabricated from several YBCO films have been tested and analyzed and a summary is presented in Table I. A few properties should be emphasized here. The resistivity of the current YBCO films at room temperature is larger compared to the results published previously [10]. High resistance bolometers show larger responsivity as discussed in [10] and confirmed in [8]. However if the device impedance is too large, the RF mismatch between the antenna and the detector becomes significant leading to a reduction of the coupling efficiency.

The thermal boundary resistance, R_{bd}, value is in the range from 0.5 to 3 × 10^{-4} cm^{2}K/W and in the same order of magnitude as previously reported [10]. We explain the observed scattering of the $R_{\rm bd}$ value by a nonuniform interface quality between the film and the substrate. Further research is ongoing in order to optimize the film deposition parameters and improve the thermal boundary resistance reproducibility.

V. Responsivity

The optical responsivity measured in a number of YBCO nano-bolometers as a function of the bias current is shown in Fig. 3. For these measurements the detector was placed close to the source horn as described in Section III. The maximum optical responsivity measured for the optimum optical alignment and at 1 mA bias current was 45 V/W in a device with a bolometer area of 0.15 μm^2. The measured responsivity values include the calibration factors discussed in the experimental setup section.

Previously we have shown [10] that for large devices the responsivity scales linearly with the bias current in a large range of currents. However, for nano-bolometers a sub-linear dependence with the bias current was observed above 0.6 mA (see Fig. 3). In order to verify whether the nonlinear dependence of $R_V(i)$ is due to an overheating, a high RF power was applied

TABLE I
FILM DEPOSITION TEMPERATURE (T_D), DEVICE SIZE ($w \times l$), ROOM TEMPERATURE RESISTANCE (R_{300}), TEMPERATURE COEFFICIENT OF RESISTANCE (TCR), THERMAL CONDUCTANCE (G), RESISTIVITY (ρ_{300}), DC RESPONSIVITY (R_V), OPTICAL RESPONSIVITY ($R_{\rm opt}$), SQUARED ANTENNA-BOLOMETER REFLECTION COEFFICIENT (Γ^2)

Device	T_D	w×l(μm^2)	R_{300}(Ω)	TCR(K^{-1})	G(μW/K)	ρ_{300}(μΩ×cm)	Rv(V/W) at 0.2mA	R_{opt}(V/W) at 0.2mA	R_{opt}/Rv at 0.2mA	Γ^2	$R_{opt}/(1-\Gamma^2)$ at 0.2mA
S14-7	780	0.3x0.5	859	0.0015	14	3600	21.8	12.8	0.58	0.6	32
S14-6	780	0.8x0.8	600	0.0014	21	4200	8.8	2.4	0.27	0.5	4.8
S14-4	780	0.3x0.3	590	0.0012	13	4130	11.6	9.4	0.81	0.5	18.8
S14-8	780	0.3x0.3	650	0.0013	18	4500	12	-	-	0.54	-
S13-7	820	0.3x0.5	383	0.0022	12	1600	13	-	-	0.3	-
S6-7	835	0.3x0.5	915	-*	-*	3840	47.4	11.9	0.25	0.65	34
S18-3	835	0.3x0.5	270	0.0025	10	1130	14	-	-	0.2	-

* (G and TCR of device S6-7 is not reported because the R-T was not measured before start the RF measurements and after RF tests the device was damaged.)

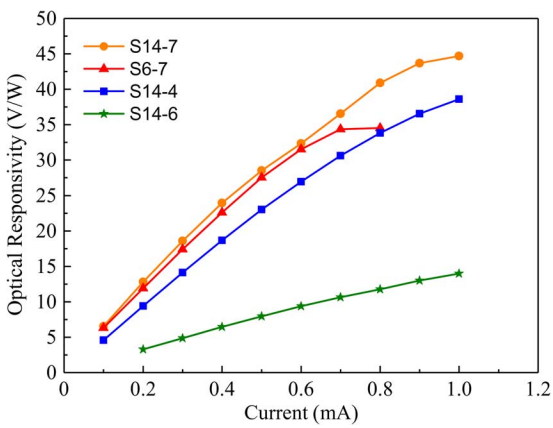

Fig. 3. Measured responsivity as a function of bias current at 400 GHz. Device details and dc responsivity (at 1 mA bias current) are presented in Table I.

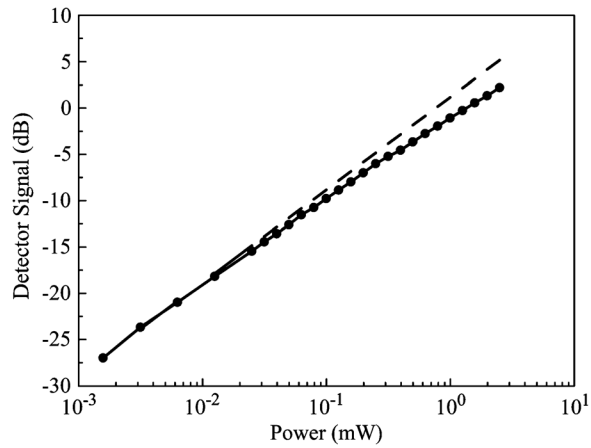

Fig. 4. Measured detector signal (symbols) as a function of the absorbed RF power. The dashed black line is a guide for the linearity behavior.

to one of the device using a 100 GHz source. The RF power absorbed in the bolometer was higher than the highest dc power used for the same sample (based on the dc resistance change).

The result showed that the sub-linear regime starts at the same bias current both with and without the RF power applied. Therefore, the sub-linear behavior of the responsivity with the current is not caused by the temperature rise in the bolometer. Furthermore, no nonlinear effects could be observed on $P_{\rm dc}/R$ curves (as in Fig. 2) up to the highest bias currents.

Linearity of the nano-bolometer response (device S18-3) to the input signal power was experimentally verified up to 2.5 mW (100 GHz) (Fig. 4). At the highest power level the signal compression was 3 dB, and the 1 dB compression was observed for the absorbed power of about 0.1–0.3 mW. The absorbed THz power was estimated from the devices voltage response and the intrinsic responsivity.

In Table I, besides the devices parameters, a comparison of the dc and the optical responsivity is also presented. The ratio between the optical and the electrical responsivities ($R_{\rm opt}/R_v$) clearly shows a reduction of the measured responsivity between 20% and 70%. This reduction appears to be mostly due to the antenna-bolometer impedance mismatch. Indeed, devices show a dc resistance (same as the RF impedance) ranging from 270 to 915 Ω. The reflection coefficient (Γ) was calculated considering the antenna impedance approximately to be 100 Ω (microwave simulations). The coupling efficiency ($\eta = 1-\Gamma^2$), antenna-bolometer, turn out to be 80% and 50% for the lower and the higher bolometer DC resistance, respectively. After the optical responsivity is corrected for the coupling efficiency a better agreement with the dc responsivity is observed. The remaining difference between the optical and the electrical responsivities can be explained by an uncertainty of the measurements.

The YBCO bolometer responsivity measured at 700 GHz and 1.6 THz (FIR gas laser) and at 100 GHz (a Gunn oscillator) are presented in Table II. The beam coupling from the laser to the bolometer was achieved using plastic lenses. The incident power was measured with a quasi-optical power meter (Thomas Keating), which unfortunately did not provide a stable power reading. For the responsivity calculation it was assumed that all the power emitted from the sources was coupled into the bolometers. Therefore, the responsivity values given in Table II are rather their lower limits. It also appears that the measured responsivity at 700 GHz is much lower compared to the responsivity measured at 400 GHz and for the same bias current. Thus

TABLE II
DEVICE SIZE ($w \times l$), ROOM TEMPERATURE RESISTANCE (R_{300}), RESISTIVITY (R_{300}), OPTICAL RESPONSIVITY ($R_{\rm opt}$), SOURCE FREQUENCY

Device	w×l(μm²)	R_{300}(Ω)	ρ_{300}(μΩ×cm)	R_{opt}(V/W) at 1mA	Frequency (THz)
S6-7	0.3x0.5	915	3840	4.8	1.6 *
S5-1	0.5x0.5	440	3080	1.8	1.6 *
S5-1	0.5x0.5	440	3080	4	0.7 *
S5-1	0.5x0.5	440	3080	9.6	0.115 **

* FIR laser power ∼ 1 mW.

** Gunn oscillator power ∼ 10 mW

it is certain that not all the power from the laser was coupled into the bolometers.

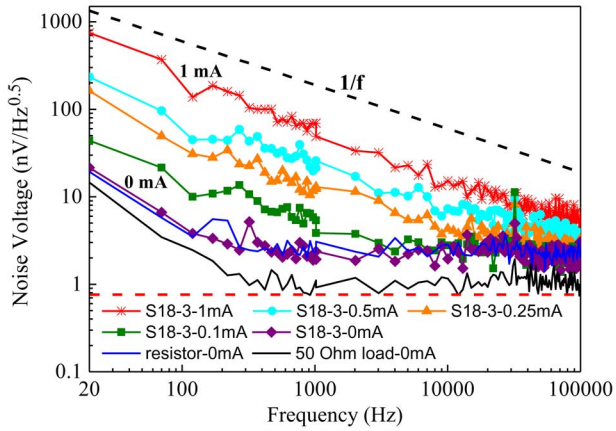

Fig. 5. Noise spectra versus modulation frequency of 0.5μm $\cdot$ 0.3μm YBCO bolometer with 270 Ω room temperature resistance at different bias currents. $1/f$ guideline (black dashed line), readout noise (red dashed line), 50 Ω load noise (black solid line), and 270 Ω resistor noise (blue solid line line).

VI. NOISE IN BIASED NANO- BOLOMETERS

The ultimate sensitivity measure of direct detectors is the noise equivalent power (NEP) which is the ratio of the voltage noise (V_N) and the responsivity (R_V) [18]. The dominant noise contributions in a bolometer are the thermal (Johnson) noise, the phonon noise and, often but not always, the low frequency flicker noise ($1/f$ noise). The Johnson noise (V_{NJ}), generated by the thermal agitation of the charge carriers, is dependent on the device resistance, R and the temperature, T. This noise source is frequency independent [see (4)]. The phonon noise (V_{NF}) is dependent on the thermal conductance G, thus how well the device is thermally isolated from the surroundings, the temperature and the responsivity. The frequency dependence of this noise source follows the one of the responsivity [see (5)]. The frequency dependence of the flicker noise ($F(f)$ in (6)) follows the $1/f$ frequency trend: $F(f) = f^{-\gamma}$, where γ is close to 1 in most cases, however, can still vary [19]. The N_N term specifies the strengths of the noise. The i^x term indicates that the flicker noise is bias current dependent. The $(1/f)$ noise is the result of many noise sources, meaning that there are no ways to estimate it beforehand and experimental measurements are usually needed. Equation (7) gives the total NEP as follows:

$$V_{NJ} = \sqrt{4RkT} \tag{4}$$

$$V_{NF} = \sqrt{4kT^2G} \cdot R_V \tag{5}$$

$$V_{NFL} = N_N i^x F(f) \tag{6}$$

$$\mathrm{NEP}^2 = \frac{V_N^2}{R_V^2} = \frac{V_{NJ}^2 + V_{NF}^2 + V_{NFL}^2}{R_V^2} = \frac{4RkT}{R_V^2} + 4kT^2G + \frac{N_N^2 i^{2x} F(f)^2}{R_V^2}. \tag{7}$$

In our work, the noise voltage of YBCO bolometers was measured from 20 Hz up to 100 kHz, as discussed in Section IV. We verified that the voltage response as a function of the modulation frequency was approximately flat for all devices in this frequency range (see Fig. 7).

Fig. 5 shows the noise spectra of a 0.5μm $\times$ 0.3μm (S18-3) YBCO bolometer. The $(1/f)$ noise guideline and the readout noise (~ 0.73 nV/Hz$^{0.5}$) lines are presented as well as the noise of 50 Ω load at zero bias (solid black line). In order to verify the accuracy of the experimental setup the noise of a 270 Ω resistor (solid blue line) was also measured showing an agreement with the theoretical prediction of the Johnson noise [2.1 nV/Hz$^{0.5}$ can be obtained from (4)]. The $(1/f)$ noise in black and blue curves below 200 Hz is hence coming from the lock-in amplifier. Using device parameters from Table I ($R = 270\Omega$, $G = 10$ μW/K, $R_V = 70$ V/W) and (5) the phonon noise was estimated to be 0.5 nV/Hz$^{0.5}$. At room temperature, bolometers seems to be Johnson noise limited. On the contrary, at cryogenic operation superconducting bolometers are usually phonon noise limited [20]. This can be explained by the fact that the device responsivity at cryogenic temperature is many orders of magnitude larger compared to the device responsivity at room temperature [see (5)]. Furthermore at low temperatures the Johnson noise becomes much smaller compared to that at the room temperature [see (4)].

As is apparent from Fig. 5, the noise voltage increases proportionally to the applied bias current for frequencies where the $(1/f)$ noise dominates. For the discussed device this is the case over the whole frequency range up to 100 kHz modulation frequency and for bias currents of 0.5 and 1 mA. However at lower bias currents (0.1 and 0.25 mA) and modulation frequencies greater than 4 kHz and 14 kHz, the noise spectrum tends to be constant and the device is limited by the thermal noise. At a 1 mA bias current and a 100 kHz modulation frequency the system noise was measured to be 4–5 nV/Hz$^{0.5}$ (see Fig. 5). For an electrical responsivity of 70 V/W (at 1 mA) the resulting system noise equivalent power was NEP $=$ 70 pW/Hz$^{0.5}$, which is a factor of 8 smaller than what we previously reported for larger bolometers [10]. By subtracting the readout noise the bolometer noise equivalent power was calculated to be $\sim$ 50 pW/Hz$^{0.5}$.

As it has been discussed in [19] and others, the $(1/f)$ noise voltage in resistive films normalized to the dc voltage drop over the sample and the film volume is more or less constant for a given material. However, in our case over a large variety of devices we observe that the volume plays no role. To start with, Fig. 6 shows the voltage-normalized noise voltage of the same device S18-3 for same bias currents as in Fig. 5. The curves overlap very well in the whole frequency range, although at low

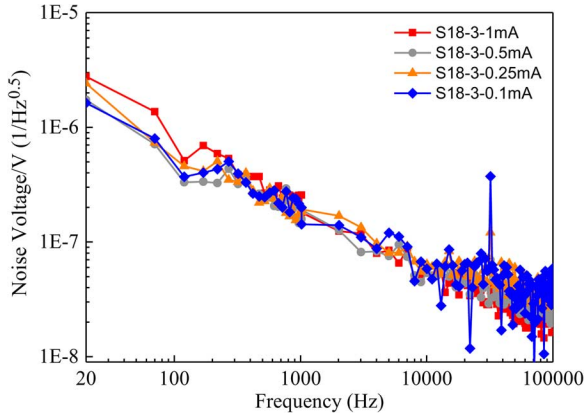

Fig. 6. Noise voltage normalized to the voltage drop over the bolometer as a function of the modulation frequency for S18-3 YBCO bolometer biased at different currents.

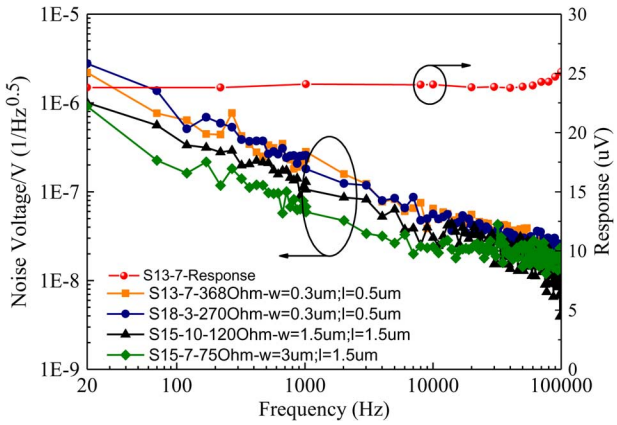

Fig. 7. Primary axis: Noise voltage normalized to the voltage drop over the bolometers as a function of the modulation frequency for bolometers made of different YBCO films, having different resistances and dimensions. Secondary axis: bolometer response as a function of the modulation frequency. Bias current was 1 mA for all devices.

frequencies the absolute noise voltages differ by up to two orders of magnitude for the currents from 0.1 to 1 mA.

It is of greater interest to compare devices of different batches and different volumes. Noise spectra of several devices normalized to the dc voltage are shown in Fig. 7. There, devices were biased at the same current (1 mA), made of different films (deposited at different parameters), with the same thickness of 70 nm, with different areas (ranging from 4.5 to 0.15 μm^2) and resistances (ranging from 368 to 75 Ω). We observe that (V_N/V) curves are almost the same for devices which differ in volume by about a factor of 30.

In Fig. 8, the noise spectra of bolometers of two film thickness are presented. The measured devices had the same bolometer area ($w = 1.5$ μm; $l = 1.5$ μm) but different film thicknesses (150 and 70 nm) and resistances (62 and 120 Ω, respectively). The TCR was measured to be 0.0014 K^{-1} for the 70 nm film and 0.002 K^{-1} for the 150 nm film. Both bolometers were biased at the same current (3.3 mA). The ratio of (V_N/V) is still the same, despite the volume difference by a factor of 2. A higher TCR for a thicker film does not appear to affect the noise voltage either.

The noise was measured on many other devices, e.g. on high resistance devices like S6-7 (see Table I), for which the voltage-

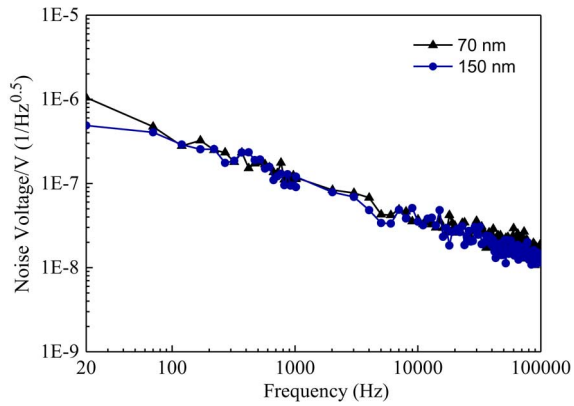

Fig. 8. Noise voltage normalized to the voltage drop over the bolometers as a function of the modulation frequency for devices with different film thicknesses and same bolometer area ($w = 1.5$ μm; $l = 1.5$ μm). Blue line: device on 150 nm film and $R = 62\Omega$. Black line: device on 70 nm film and $R = 120\Omega$.

normalized noise voltage coincided well with the data shown in Figs. 6 and 7, where $(V_N/V)^2 = 6 \times 10^{-11} \times 1/f$ Hz^{-1}. As it follows from the data above, this value of $(V_N/V)^2$ is constant over a large variation of the bolometer volumes, geometries (width to length rations), and thicknesses.

This value can be now be applied for the noise estimates for any other YBCO room temperature bolometers in the limit of the $(1/f)$ noise.

VII. Discussion

A. General Considerations

From (1) and (2), it is clear that for a given bias current and the bolometer resistance (defined by the length to the width ratio) the responsivity scales inversely with the bolometer area A. Since the smallest bolometer dimension which we discuss here is 300 nm, further reduction of the bolometer area will still be possible. Furthermore, keeping area fixed but fabricating bolometers with longer and narrower geometries the resistance will increase as well as the responsivity for the given current. However, as it has previously been discussed, the device resistance cannot be too large due to the antenna-bolometer impedance mismatch loss. Moreover, the Johnson noise will be larger for a large resistance so a tradeoff must be found.

Equation (1) for a low current regime $(G >> i^2 \times \alpha \times R)$ can be rewritten as

$$R_V = \frac{\alpha \cdot i \cdot R}{G} = \frac{\alpha \cdot V}{A} R_{\rm bd}. \tag{8}$$

Therefore, the noise equivalent power can be expressed for modulation frequencies where the $(1/f)$ noise dominates as

$$\mathrm{NEP} = \frac{V_N}{R_V} = \frac{V_N}{V}(\omega) \cdot \frac{A}{\alpha \cdot R_{\rm bd}}. \tag{9}$$

As we have experimentally shown, the ratio of the noise voltage to the device voltage drop (V_N/V) is approximately constant at each modulation frequency.

B. Operation Optimization

Since both the responsivity and the noise voltage depend on the bias current, and the noise voltage is also a function of the

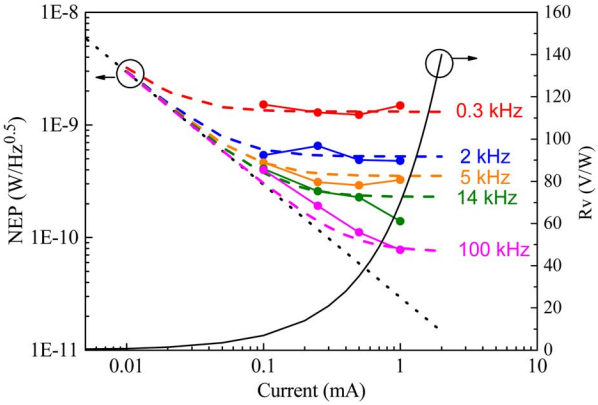

Fig. 9. Device S18-3. Noise equivalent power and electrical responsivity as a function of the bias current. Johnson and phonon noise (dotted black line). Responsivity as a function of the bias current (solid black line). Experimental NEP (filled circles). Fit to the measured data (dashed lines).

modulation frequency, let us do the following exercise. Both the noise equivalent power and the responsivity are parametrically plotted as a function of the bias current with the modulation frequency as the parameter (Fig. 9 for device S18-3). The filled circles indicate the NEP obtained from the measured data. For a chosen frequency the noise equivalent power is extrapolated from the noise voltage (Fig. 6) and the electrical responsivity. At each modulation frequency the experimental NEP was fitted using (10) (dashed lines), which shows a good agreement with the experiment (circles). Experimental data scattering is caused by the limited accuracy in the noise voltage measurements. Equation (10) was obtained from (7) and (9)

$$\mathrm{NEP}^2 = \frac{4RkT + V_{N-\mathrm{readout}}^2}{R_V^2(i)} + 4kT^2G + \left(\frac{V_N}{V}(\omega)\cdot\frac{A}{\alpha\cdot R_{bd}}\right)^2 \tag{10}$$

where $R_V(i)$ is the measured electrical responsivity as a function of the bias current (solid black line). (V_N/V) is obtained from Fig. 6, and $V_{N-\mathrm{readout}}$ is the noise of the readout circuit. Additionally, device parameters are given in Table I. The dashed black line in Fig. 9 represents the NEP limit imposed by the sum of the Johnson and the phonon noise sources. At low currents the NEP is always limited by the Johnson noise at any frequency. On the contrary, as the current increases the NEP becomes $(1/f)$ noise limited. This limit is lower for higher modulation frequencies. Therefore, if the system allows, lower NEP is reached at higher modulation frequencies.

C. Device Optimization

Due to the constant ratio of (V_N/V) in (9) for the film volume, resistivity, and TCR, a higher sensitivity (lower NEP) can be reached by minimizing the second term in (9). Apart from the device area A, it is the temperature coefficient of resistance (TCR), α, and the thermal boundary resistance, R_{bd} which allow for further optimization. Because the R_{bd} and the TCR are material dependent, either further YBCO growth optimization or utilization of other materials will be required.

Previously, we have reported mixing experiments on YBCO substrate supported bolometers. There, a response time of 2 ns ($\sim$ 65 MHz) [10] for bolometers made of thin YBCO films was demonstrated, which is the lowest time constant reported among room temperature bolometers. Regarding the response time, thicker films and higher thermal boundary resistance will increase the time constant. However, if we want to optimize the noise of YBCO bolometer (and therefore the sensitivity) at modulation frequency lower than 100 kHz, which is much lower than 65 MHz, nanoseconds response time is not needed.

This leads us to two other possible directions for the device optimization: 1) a larger TCR for YBCO could be obtained by making thicker films [21] and 2) the thermal boundary resistance could possibly be increased by modifying the interface between the YBCO film and the substrate, e.g., by thinning or thickening the buffer layer. Such investigation is now in progress. Furthermore another feasible option to tailor the R_{bd} could be to use other substrate materials [22].

VIII. Conclusion

In conclusion, YBCO bolometers made on bulk substrates are shown to be very promising candidates as room temperature THz detectors due to their large RF bandwidth (just limited by the antenna), fast response and high sensitivity.

Recent publications [12] confirm that even other materials (e.g., $PrBa_2Cu_3O_{7-x}$) can be used for similar devices with a great success.

An electrical and optical responsivity up to 230 V/W and 45 V/W, respectively, at 1 mA bias current has been measured for devices with a bolometer area of 0.15 μm^2. A minimum electrical noise equivalent power of 50 pW/Hz$^{0.5}$ has been achieved at 100 kHz modulation frequency. The $(1/f)$ noise voltage normalized over the bolometers voltage drop has been measured to be as $(V_N/V)^2 = 6 \times 10^{-11} \times 1/f$ Hz^{-1}, and it is constant for a large variety of measured devices made of different films, having different areas, resistances, and thicknesses. Using this value, the crossover frequency to the thermal noise limited operation can be calculated providing the modulation frequency optimal for an application of interest.

Further improvements of the detector, both the responsivity and the NEP, is expected by increasing the temperature coefficient of resistance, as well as increasing the thermal boundary resistance, and minimizing the device area.

References

[1] P. Siegel, "Terahertz technology," *IEEE Trans. Microw. Theory Techn.*, vol. 50, no. 3, pp. 910–928, Mar. 2002.
[2] P. Siegel, "Terahertz technology in biology and medicine," *IEEE Trans. Microw. Theory Techn.*, vol. 52, no. 10, pp. 2438–2447, Oct. 2004.
[3] F. Sizov and A. Rogalski, "THz detectors," *Progr. Quantum Electron.*, vol. 34, pp. 278–347, 2010.
[4] J. L. Hesler and T. W. Crowe, "Responsivity and noise measurements of zero-bias schottky diode detectors," in *Proc. 18th Int. Symp. on Space THz Technol.*, Mar. 2007, pp. 89–92.
[5] L. Liu, J. L. Hesler, H. Xu, A. W. Lichtenberger, and R. M. Weikle, "A broadband quasi-optical terahertz detector utilizing a zero bias Schottky diode," *IEEE Microw. Wireless Compon. Lett.*, vol. 20, no. 9, pp. 504–506, Sep. 2010.
[6] F. Schuster, D. Coquillat, H. Videlier, M. Sakowicz, F. Teppe, L. Dussopt, B. Giffard, T. Skotnicki, and W. Knap, "Broadband terahertz imaging with highly sensitive silicon CMOS detectors," *Opt. Express*, vol. 19, no. 8, pp. 7827–7832, 2011.
[7] N. Chi-Anh, H.-J. Shin, K. T. Kim, Y.-H. Han, and S. Moon, "Characterization of uncooled bolometer with vanadium tungsten oxide infrared active layer," *Sensors Act. A: Physical*, vol. 123–124, no. 23, pp. 87–91, 2005.

[8] T. Xue-Cou, K. Lin, L. Xin-Hua, M. Qing-Kai, W. Chao, C. Jian, J. Biao-Bing, J. Zheng-Ming, X. Wei-Wei, and W. Pei-Heng, " Nb_5N_6 microbolometer arrays for terahertz detection," *Chin. Phys. B*, vol. 22, no. 4, pp. 040701-1–040701-4, 2013.
[9] C. Dietlein, A. Luukanen, J. S. Penttilä, H. Sipola, L. Grönberg, H. Seppä, P. Helistö, and E. N. Grossman, "Performance comparison of Nb and NbN antenna-coupled microbolometers," in *Proc. SPIE 6549, THz for Military and Sec. Appl. V*, 2007, vol. 65490M.
[10] S. Cherednichenko, A. Hammar, S. Bevilacqua, V. Drakinskiy, J. Stake, and A. Kalabukhov, "A room temperature bolometer for coherent and incoherent detection," *IEEE Trans. THz Sci. Technol.*, vol. 1, no. 2, pp. 395–402, Nov. 2011.
[11] S. Bevilacqua and S. Cherednichenko, "Fast room temperature THz bolometers," in *Proc. 38th Infrared, Millim. THz Waves*, 2013, pp. 1–2.
[12] A. Scheuring, P. Thoma, J. Day, K. Il'in, J. Hänisch, B. Holzapfel, and M. Siegel, "Thin PrBaCuO film antenna-coupled THz bolometers for room temperature operation," *IEEE Trans. THz Sci. Technol.*, vol. 3, no. 1, pp. 103–109, Jan. 2013.
[13] J. M. Phillips, "Substrate selection for high-temperature superconducting thin films," *J. Appl. Phys*, vol. 79, no. 4, pp. 1829–1848, 1996.
[14] A. Hammar, S. Cherednichenko, S. Bevilacqua, V. Drakinskiy, and J. Stake, "Terahertz direct detection in $YBa_2Cu_3O_7$ microbolometers," *IEEE Trans. THz Sci. Technol.*, vol. 1, no. 2, pp. 390–394, Nov. 2011.
[15] F. Rönnung, S. Cherednichenko, D. Winkler, and G. Gol'tsman, "A nanoscale YBCO mixer optically coupled with a bow tie antenna," *Supercond. Sci. Technol.*, vol. 12, no. 11, pp. 853–855, 1999.
[16] P. L. Richards, J. Clarke, R. Leoni, Ph. Lerch, and S. Verghese, "Feasibility of the high Tc superconducting bolometer," *Appl. Phys. Lett.*, vol. 54, no. 3, pp. 283–285, Jan. 1989.
[17] E. T. Swartz and R. O. Pohl, "Thermal resistance at interfaces," *Appl. Phys. Lett.*, vol. 51, no. 26, pp. 2200–2202, Dec. 1987.
[18] P. L. Richards, "Bolometers for infrared and millimeter waves," *J. Appl. Phys.*, vol. 76, no. 1, 1994.
[19] R. F. Voss and J. Clarke, "Flicker $(1/f)$ noise: Equilibrium temperature and resistance fluctuations," *Phys. Rev. B.*, vol. 13, no. 2, 1976.
[20] J. C. Mather, "Bolometer noise: Nonequilibrium theory," *Appl. Opt.*, vol. 21, no. 6, pp. 1125–1129, 1982.
[21] J. A. Greer, "High quality YBCO films grown over large areas by pulsed laser deposition," *J. Vac. Sci. Technol. A*, vol. 10, no. 4, pp. 1821–1826, 1992.
[22] C. D. Marshall, A. Tokmakoff, I. M. Fishman, C. B. Eom, J. M. Phillips, and M. D. Fayer, "Thermal boundary resistance and diffusivity measurements on thin $YBa_2Cu_3O_{7x}$ films with MgO and $SrTiO_3$ substrates using the transient grating method," *J. Appl. Phys.*, vol. 73, no. 2, pp. 850–857, 1993.

Stella Bevilacqua was born in 1981 in Pizza Armerina, Italy. She received B.Sc. degree in electronic engineering from the University of Catania, Italy, in 2006, and the M.Sc. degree in microelectronic engineering from the University of Catania, in April 2010. She was a diploma worker at Chalmers University of Technology in the Department of Microtechnology and Nanoscience, where she was working towards her master thesis: 'Fabrication and Characterization of Graphene field-effect transistors (GFETs)', for a six-month period. Currently, she is working toward the Ph.D. degree from the Department of Terahertz Millimeter Wave Laboratory, Chalmers University of Technology, Goteborg, Sweden, working on MgB2 and YBCO Hot Electron Bolometers.

During a four-month period, she did her thesis work in the Smart-Card group of the MPG division of Catania STMicroelectronics.

Sergey Cherednichenko was born in Mariupol, Ukraine, in 1970. He received the Diploma (with Hons) in physics from Taganrog State Pedagogical Institute, in 1993, and the Ph.D. degree in physics from Moscow State Pedagogical University, in 1999.

He is working at the Department of Microtechnology and Nanoscience at Chalmers University of Technology (Gothenburg, Sweden). From 2000 to 2006, he was involved in development of terahertz band superconducting mixers for the Herschel Space Observatory; and from 2008 till 2009, in the water vapor radiometer for ALMA. From 2007, he is Associate Professor at the Department of Microtechnology and Nanoscience, Chalmers University of Technology, Goteborg, Sweden. His research interests include terahertz heterodyne receivers and mixers, photon detectors; THz antennas and optics; thin superconducting films and their application for THz and photonics; and material properties at THz frequencies.